Absolute Binding Energies of Lithium Ions to Short Chain Alcohols, $C_nH_{2n+2}O$, $n = 1-4$, Determined by Threshold Collision-Induced Dissociation

M. T. Rodgers and P. B. Armentrout*

Department of Chemistry, University of Utah, Salt Lake City, Utah 84112

Received: January 7, 1997[⊗]

Collision-induced dissociation of Li^+(ROH) with xenon is studied using guided ion beam mass spectrometry. ROH includes the following eight short chain alcohols: methanol, ethanol, 1-propanol, 2-propanol, 1-butanol, 2-methyl-1-propanol, 2-butanol, and 2-methyl-2-propanol. In all cases, the primary product is endothermic loss of the neutral alcohol, with minor products that include those formed by ligand exchange, alkene and water loss, and C−C bond cleavage. The cross-section thresholds are interpreted to yield 0, 298, and 373 K bond energies for Li^+−ROH after accounting for the effects of multiple ion−molecule collisions, internal energy of the reactant ions, and dissociation lifetimes. The experimental bond energies determined here show a fairly constant deviation from previous experimental measurements (as obtained by equilibrium studies in an ion cyclotron resonance mass spectrometer). This discrepancy is discussed in some detail because it affects the absolute Li^+ affinity scale used extensively in the literature.

Introduction

Noncovalent metal−ligand interactions are a primary influence on the three-dimensional structures of biological molecules, which in turn help determine their functionality. Quantitative studies in the gas phase provide one way of obtaining more detailed information on such effects because the individual interactions can be easily isolated. In the present study, we examine a simple metal−ligand system that can act as a fundamental model for noncovalent metal−ligand interactions: Li^+(ROH), where ROH = methanol (MeOH), ethanol (EtOH), 1-propanol (*n*-PrOH), 2-propanol (*i*-PrOH), 1-butanol (*n*-BuOH), 2-methyl-1-propanol (*i*-BuOH), 2-butanol (*s*-BuOH), and 2-methyl-2-propanol (*t*-BuOH). In addition, these systems form an intrinsically interesting sequence in which the size and geometry of the alkyl group provide a systematic influence on the binding energies.

In this work, we directly measure the absolute bond dissociation energies (BDEs) of the Li^+(ROH) species using guided ion beam mass spectrometry. This technique enables us to examine the kinetic energy dependence of collision-induced dissociation (CID) reactions of the Li^+(ROH) complexes. Although this method has seen reasonable success for a variety of small metal−ligand complexes,[1−5] as the size of the molecule increases, the dissociation efficiency at the thermodynamic threshold should decrease because internal energy randomization can increase the lifetime of the energized molecule until it exceeds the experimental time window available. This results in a kinetic shift, a reduced sensitivity for measuring the true thermodynamic onset for the CID process, that becomes more noticeable as the size of the molecule increases.[6] Thus, the Li^+-(ROH) sequence of complexes provides a possible test of the methods we have used to estimate this lifetime effect[1] because the extent of the kinetic shift should increase systematically with the size of the alcohol. This test is further enhanced because thermodynamic data on these complexes has been previously obtained by equilibrium studies.[7]

Previous work designed to measure the Li^+ binding affinities of various bases has included several techniques. Chief among these are equilibrium studies, in either an ion cyclotron resonance (ICR) mass spectrometer or a high-pressure mass spectrometer (HPMS), Cook's kinetic method[8] in a tandem mass spectrometer, and energy-resolved CID studies. The binding energies of Li^+ to multiple H_2O ligands have been studied using HPMS by Dzidic and Kebarle (DK)[9] and by the present authors using CID methods.[10] The binding energies of Li^+ to various bases, including the alcohols of direct interest here, have been studied by equilibrium methods in an ICR by Beauchamp and co-workers[11,12] and by Taft et al.[7] Cook's kinetic method has been used to determine the Li^+ binding affinities of the commonly occurring amino acids[13] and nucleic acid bases.[14] CID methods have been utilized to study the binding of Li^+ to various ether complexes, including acyclic as well as crown ethers,[2,3] and to CO.[15] We have also measured the Li^+ binding affinities of the nucleic acid bases as well as other molecules of biological importance, results that will be presented elsewhere.[16]

Despite this abundance of relevant information, a direct comparison between the present results and those of the literature is flawed by two considerations. First, Taft et al.[7] calibrated their relative Li^+ affinity scale by adjusting values determined by Woodin and Beauchamp[12] for differing experimental temperatures. As we discuss in some detail below, it appears that this calibration was performed incorrectly. Second, the absolute Li^+ affinities reported in Taft's equilibrium study (as well as other studies throughout the literature) can be traced back to the value of $D(Li^+-OH_2)$ reported by DK.[9] This bond energy was not measured directly but was extrapolated from measurements made for larger $Li^+(H_2O)_n$ clusters. In another study, we recently made the first direct measurement of the Li^+-OH_2 bond energy.[10] Results of this study suggest that the Li^+-OH_2 bond energy estimated by DK was too high. This result and the flawed temperature correction imply that a systematic reduction of all Li^+ affinities that used these values as references is in order.

In the process of investigating the resultant discrepancy, we reexamined some of the fundamental assumptions that we used to estimate the lifetime effects in collisionally activated decompositions. This has led to a revised method of estimating parameters needed for the RRKM analysis used to determine kinetic shifts and is discussed in detail elsewhere.[17] We believe that this method removes much of the guesswork associated with choosing molecular parameters for the dissociation transi-

[⊗] Abstract published in *Advance ACS Abstracts,* March 1, 1997.

S1089-5639(97)00154-0 CCC: $14.00

tion state and also places the incorporation of unimolecular decomposition theory into our analysis of CID processes on a firmer theoretical basis. The present work provides some empirical justification for this revised procedure.

Experimental Section

General Procedures. Cross sections for CID of lithiated alcohols are measured using a guided ion beam mass spectrometer which has been described in detail previously.[18,19] The metal ion bound alcohols are generated as described below. The ions are extracted from the source, accelerated, and focused into a magnetic sector momentum analyzer for mass analysis. Mass-selected ions are decelerated to a desired kinetic energy and focused into an octopole ion guide which traps the ions in the radial direction.[20] The octopole passes through a static gas cell containing xenon, used as the collision gas, for reasons described elsewhere.[4,21,22] Low gas pressures in the cell (typically 0.03−0.20 mTorr) are used to ensure that multiple ion−molecule collisions are improbable. Product and unreacted beam ions drift to the end of the octopole where they are focused into a quadrupole mass filter for mass analysis and subsequently detected with a secondary electron scintillation detector and standard pulse counting techniques.

Ion intensities are converted to absolute cross sections as described previously.[18] Absolute uncertainties in cross section magnitudes are estimated to be ± 20%, which is the largely the result of error in the pressure measurement and the length of the interaction region. Relative uncertainties are approximately ±5%. Because the radio frequency used for the octopole does not trap light masses with high efficiency, the cross sections for Li^+ products were more scattered and showed more variations in magnitude than is typical for this apparatus. Therefore, absolute magnitudes of the cross sections for production of Li^+ are probably ±50%. We verified that the energy dependences (and thus the threshold analyses) of the Li^+ product cross sections were not affected by these variations in magnitude.

Ion kinetic energies in the laboratory frame, E_{Lab}, are converted to energies in the center-of-mass frame, E_{CM}, using the formula $E_{CM} = E_{Lab}m/(m + M)$, where M and m are the masses of the ionic and neutral reactants, respectively. All energies reported below are in the CM frame unless otherwise noted. The absolute zero and distribution of the ion kinetic energies are determined using the octopole ion guide as a retarding potential analyzer as previously described.[18] The distribution of ion kinetic energies is nearly Gaussian with a fwhm typically between 0.2 and 0.3 eV (Lab) for these experiments. The uncertainty in the absolute energy scale is ± 0.05 eV (Lab).

Even when the pressure of the reactant neutral is low, we have previously demonstrated that the effects of multiple collisions can significantly influence the shape of CID cross sections.[5] Because the presence and magnitude of these pressure effects are difficult to predict, we have performed pressure-dependent studies of all cross sections examined here. Data free from pressure effects can always be obtained by extrapolating to zero pressure, as described previously.[5] In all systems studied here, we found no dependence on Xe pressure up to the highest pressure examined, ∼0.2 mTorr. Thus, results reported here are due to single bimolecular encounters.

Ion Source. The lithiated alcohols are formed in a 1 m long flow tube[19,23] operating at a pressure of 0.5−0.7 Torr with a helium flow rate of 4000−7000 sccm. Metal ions are generated in a continuous dc discharge by argon ion sputtering of a cathode, made from tantalum or iron, with a cavity containing lithium metal. Typical operating conditions of the discharge are 1.5−3 kV and 20−30 mA in a flow of roughly 10% argon in helium. The lithiated alcohols are formed by associative reactions of the lithium ion with the neutral alcohols which are introduced into the flow 50 cm downstream from the dc discharge. The flow conditions used in this ion source provide in excess of 10^4 collisions between an ion and the buffer gas, which should thermalize the ions both vibrationally and rotationally. In our analysis of the data, we assume that the ions produced in this source are in their ground electronic states and that the internal energy of the lithiated alcohols is well described by a Maxwell−Boltzmann distribution of ro-vibrational states corresponding to 300 K. Previous work from this laboratory has shown that these assumptions are generally valid.[1,4,5,23−26]

Thermochemical Analysis. The threshold regions of the reaction cross sections are modeled using eq 1,

$$\sigma = \sigma_0 \sum_i g_i (E + E_i - E_0)^n / E \qquad (1)$$

where σ_0 is an energy-independent scaling factor, E is the relative translational energy of the reactants, E_0 is the threshold for reaction of the ground electronic and ro-vibrational state, and n is an adjustable parameter. The summation is over the ro-vibrational states of the reactant ions, i, where E_i is the excitation energy of each state and g_i is the population of those states ($\sum g_i = 1$). The populations of excited ro-vibrational levels are not negligible even at 300 K as a result of the many low-frequency modes present in these ions. It is assumed that n and σ_0 in eq 1 are the same for all states.

Semiempirical calculations were performed with Hyperchem[27] to obtain model structures, energetics, and vibrational frequencies for the neutral and lithiated alcohols. Calculations were performed using the PM3[28−30] method. In all of the calculations, starting structures are annealed and then energy minimized. A vibrational analysis of the geometry-optimized structures is then performed to determine the vibrational frequencies and rotational constants of the molecules. Results of a recent literature study[31] indicate that frequencies computed using the semiempirical PM3 method compare well to values obtained at the *ab initio* level using medium-sized basis sets. Of all semiempirical methods, PM3 showed the closest correspondence to *ab initio* and experimental values. Because this literature study involved only covalently bonded compounds, we performed *ab initio* calculations at the 6-31G** level on several of the Li^+-alcohol complexes to compare the vibrational frequencies obtained at this level to those obtained using the semiempirical PM3 method. We found comparable frequencies with both semiempirical and *ab initio* methods even for the vibrational modes corresponding to Li^+−alcohol noncovalent interactions. Similar results were found for Li^+ crown ether complexes, pertinent to another study.[3] Studies over the past two decades have established that the discrepancy between the computed and experimental force constants is sufficiently systematic to allow the application of generalized scaling procedures which bring the computed vibrational spectrum into agreement with experiment.[32] Computed vibrational frequencies determined at the semiempirical level of theory are typically 10% too high. We have therefore scaled the vibrational frequencies obtained in our analyses by a factor of 0.9. The scaled vibrational frequencies thus obtained using the PM3 method for the neutral and lithiated alcohols are listed in Table 1. Rotational constants of all complexes are listed in Table 2. The Beyer−Swinehart algorithm[33,34] is used to calculate the population distribution of ro-vibrational states using these frequencies and rotational constants.

The average vibrational energy at 298 K of the neutral and lithiated alcohols is also given in Table 1. We have estimated

TABLE 1: Vibrational Frequencies and Average Vibrational Energies at 298 K[a]

species	$E_{vib,}$[b] eV	frequencies, cm^{-1}
MeOH	0.02 (0.01)	255, 889, 918, 1047, 1225, 1229 (2), 1267, 2733, 2762, 2828, 3507
Li^+(MeOH)	0.07 (0.01)	**92**, **135**, 307, **392**, 877, 901, 990, 1180, 1197, 1209, 1229, 2730, 2738, 2773, 3468
EtOH	0.05 (0.02)	153, 275, 416, 752, 869, 918, 990, 1003, 1017, 1197, 1239, 1245, 1267, 1269, 1280, 2646, 2728, 2775, 2783, 2868, 3500
Li^+(EtOH)	0.09 (0.02)	**96**, **195**, 216, 246, **347**, 454, 754, 839, 915, 961, 972, 1006, 1131, 1174, 1213, 1225, 1265, 1280, 2635, 2672, 2678, 2688, 2816, 3485
n-PrOH	0.09 (0.02)	87, 158, 248, 321, 459, 740, 813, 845, 918, 935, 993, 1016, 1026, 1044, 1178, 1209, 1240, 1253, 1265, 1266, 1270, 1285, 2645, 2661, 2724, 2734, 2773, 2777, 2864, 3498
Li^+(*n*-PrOH)	0.12 (0.03)	**90**, 145, **185**, 255, 288, 313, **380**, 463, 721, 792, 834, 885, 911, 962, 1005, 1017, 1018, 1148, 1169, 1179, 1216, 1229, 1244, 1265, 1292, 2634, 2640, 2657, 2677, 2681, 2730, 2813, 3472
i-PrOH	0.09 (0.03)	132, 157, 210, 348, 402, 462, 839, 858, 874, 880, 987, 992, 1021, 1099, 1200, 1237, 1260, 1263, 1266, 1270, 1273, 1295, 2549, 2775, 2778, 2781, 2782, 2865, 2866, 3512
Li^+(*i*-PrOH)	0.13 (0.03)	**69**, 142, **175**, 215, 281, **334**, 350, 452, 469, 815, 851, 857, 867, 956, 987, 1021, 1092, 1127, 1214, 1227, 1248, 1254, 1261, 1274, 1281, 2555, 2675, 2694, 2769, 2771, 2816, 2858, 3476
n-BuOH	0.12 (0.03)	65, 92, 168, 227, 285, 340, 487, 704, 788, 812, 863, 913, 935, 988, 1012, 1017, 1025, 1036, 1052, 1130, 1202, 1232, 1241, 1252, 1264, 1269, 1270, 1275, 1290, 2645, 2653, 2664, 2723, 2730, 2733, 2771, 2777, 2864, 3498
Li^+(*n*-BuOH)	0.17 (0.04)	**52**, 113, 133, **212**, 279, 285, 307, 375, **382**, 444, 721, 748, 801, 834, 885, 919, 931, 967, 1000, 1026, 1032, 1041, 1130, 1164, 1172, 1202, 1222, 1234, 1249, 1260, 1262, 1284, 2609, 2639, 2646, 2650, 2656, 2687, 2718, 2728, 2805, 3470
i-BuOH	0.13 (0.03)	74, 152, 169, 245, 277, 344, 408, 468, 811, 819, 861, 877, 883, 936, 1004, 1021, 1030, 1046, 1144, 1180, 1216, 1239, 1255, 1263, 1265, 1267, 1270, 1273, 1277, 2584, 2641, 2722, 2771, 2772, 2775, 2776, 2860, 2862, 3497
Li^+(*i*-BuOH)	0.17 (0.04)	**72**, 126, 160, **179**, 232, 264, 306, 360, **374**, 422, 454, 781, 813, 859, 866, 877, 898, 961, 1006, 1013, 1039, 1112, 1164, 1167, 1195, 1216, 1223, 1255, 1258, 1261, 1268, 1292, 2584, 2638, 2639, 2677, 2679, 2773, 2774, 2808, 2860, 3471
s-BuOH	0.12 (0.03)	121, 170, 203, 212, 300, 393, 398, 476, 748, 806, 885, 895, 925, 983, 999, 1013, 1026, 1037, 1090, 1158, 1216, 1247, 1257, 1261, 1267, 1271, 1275, 1287, 1292, 2547, 2667, 2729, 2740, 2752, 2779, 2780, 2851, 2854, 3513
Li^+(*s*-BuOH)	0.17 (0.04)	**91**, 106, 157, **183**, 239, 279, 296, 317, **407**, 434, 500, 734, 791, 848, 882, 911, 938, 989, 1007, 1016, 1021, 1093, 1125, 1186, 1221, 1236, 1243, 1251, 1261, 1262, 1272, 1293, 2558, 2633, 2656, 2676, 2728, 2767, 2773, 2813, 2858, 3453
t-BuOH	0.13 (0.04)	124, 161, 166, 259, 310, 317, 406, 447, 452, 795, 855, 859, 868, 872, 902, 905, 1076, 1144, 1200, 1242, 1253, 1262, 1263 (2), 1265, 1269, 1272, 1273, 1298, 2775 (2), 2779 (2), 2781 (2), 2863, 2864, 2865, 3510
Li^+(*t*-BuOH)	0.17 (0.04)	**62**, 129, 155, **185**, 203, 292, 300, 320, **371**, 412, 436, 491, 779, 822, 846, 850, 874, 892, 899, 1062, 1117, 1159, 1214, 1232, 1247, 1250, 1253, 1256, 1259, 1262, 1273, 1282, 2681, 2690, 2769 (2), 2771, 2773, 2816, 2857 (2), 3477

[a] Vibrational frequencies are obtained from a vibrational analysis of the geometry-optimized structures for these species using the PM3 method after scaling by 0.9. The metal−ligand stretch and bends corresponding to the transitional modes are indicated in boldface with the largest of these values corresponding to the reaction coordinate. [b] Uncertainties listed in parentheses are determined as described in the text.

TABLE 2: Rotational Constants of Li^+(ROH) in cm^{-1}

	energized molecule		transition state		
alcohol	1-D[a]	2-D[b]	1-D[a]	2-D[b]	1-D[c]
MeOH	1.41	0.33	0.98	0.053	0.80, 4.18
EtOH	0.39	0.22	0.30	0.038	0.27, 1.14
n-PrOH	0.24	0.13	0.16	0.030	0.14, 0.45
i-PrOH	0.26	0.13	0.18	0.031	0.16, 0.29
n-BuOH	0.16	0.085	0.11	0.025	0.085, 0.26
i-BuOH	0.19	0.081	0.12	0.025	0.089, 0.26
s-BuOH	0.17	0.086	0.097	0.025	0.088, 0.26
t-BuOH	0.15	0.10	0.15	0.025	0.15, 0.16

[a] Active external. [b] Inactive external. [c] Rotational constants of transitional modes treated as free internal rotors.

the sensitivity of our analysis to the deviations from the true frequencies by scaling the originally calculated PM3 frequencies to encompass the range of average valence coordinate scale factors needed to bring calculated frequencies into agreement with experimentally determined frequencies found by Seeger et al.[31] All of the originally calculated vibrational frequencies were scaled by 0.7 and 1.1. The corresponding change in the average vibrational energy is taken to be an estimate of one standard deviation of the uncertainty in vibrational energy and is included in the uncertainties of E_0.

Another consideration in the analysis of CID thresholds is whether dissociation occurs within the time scale of the experiment, approximately 10^{-4} s in our instrument. If the lifetime of the collisionally excited ion exceeds this, then a kinetic shift will be observed as an increase in the apparent thresholds to higher kinetic energies. This effect is included in our threshold analysis by incorporating RRKM theory in eq 1, as has been described in detail elsewhere.[1,17,35] Briefly, eq 1 is integrated over a dissociation probability determined from the set of ro-vibrational frequencies appropriate for the energized molecule and the transition state (TS) leading to dissociation. These frequencies are derived from the frequencies and rotational constants listed in Tables 1 and 2. Choices for the molecular parameters of the TS can be estimated with two limiting assumptions and a choice that reflects the most probable TS. In the first limit, lifetime effects are ignored. (In essence, this assumes that the rate of dissociation at all collision energies is faster than the experimental timescale.) At the other extreme, the most reasonable upper limit to the kinetic shift is provided by a tight TS, where the molecular parameters of the TS are assumed to equal those of the dissociating molecule minus the single mode that corresponds to the reaction coordinate. The reaction coordinate (the highest frequency identified by boldface type in Table 1) is associated with the Li−O stretch. Because the interaction between the lithium ion and the alcohol is largely electrostatic, the most appropriate model for estimating the lifetime effect should be a loose TS. In this case, the TS vibrations used are the frequencies corresponding to the free alcohol and are listed in Table 1. The transitional frequencies, those that become rotations of the completely dissociated products, are treated as rotors, a treatment that corresponds to a phase space limit (PSL) and is described in detail elsewhere.[17]

For the Li^+(ROH) complexes, the two transitional mode rotors have rotational constants equal to those of the ROH product with axes perpendicular to the reaction coordinate. These are listed in Table 2. The external rotations of the energized molecule and TS are also included in the modeling of the CID data. The external rotational constants of the TS are determined by assuming that the TS state occurs at the centrifugal barrier for interaction of Li^+ with ROH, calculated using the formulas listed by Khan et al.[1] that are based on a treatment of Waage and Rabinovitch (WR).[36] The geometry of the dissociating Li^+-(ROH) complex is then adjusted to include this extended Li^+−ROH bond distance, and the rotational constants are calculated. If the Li^+ is moved away from the alcohol along the line connecting the centers of masses of these species, then the 1-D rotational constant is unaffected and the 2-D rotational constant is reduced. However, we thought it more appropriate to move the Li^+ away along the Li^+−O direction because the electrostatic interaction is mainly localized between the lithium ion and the oxygen atom. The external rotational constants of the transition state determined using this method are listed in Table 2. In this method, both the external 1-D and 2-D rotors change in going from the energized molecule to the TS, although the 1-D rotor is not affected greatly. We verified that the threshold analyses were not significantly affected by these variations in the rotational constants of the TS (changes in E_0 of less than 0.01 eV). The 2-D external rotations are treated adiabatically but with centrifugal effects included consistent with the discussion of WR,[36] although statistical assumptions appropriate for collisional activation are included. These assumptions are discussed in detail elsewhere.[17] This paper also describes the derivation of a variational approach that locates the TS for dissociation of an ion−molecule complex at the centrifugal barrier. This approach leads to threshold energies that differ from those using the method described above by less than 0.01 eV in all Li^+−ROH systems examined here.

The model represented by eq 1 is expected to be appropriate for translationally driven reactions.[37] This model form has been found to reproduce reaction cross sections well in a number of previous studies of both atom−diatom and polyatomic reactions,[38,39] including CID processes.[1−5,23] The model is convoluted with the kinetic energy distribution of the reactants, and a nonlinear least-squares analysis of the data is performed to give optimized values for the parameters σ_0, E_0, and n. The error associated with the measurement of E_0 is estimated from the range of threshold values determined for different data sets, variations associated with uncertainties in the vibrational frequencies, and the error in the absolute energy scale, 0.05 eV (Lab). For analyses that include the RRKM lifetime effect, the uncertainties in the reported E_0 values also include the effects of increasing and decreasing the time assumed available for dissociation (10^{-4} s) by a factor of 2 and the sensitivity of our analysis to the values for the transitional modes (ascertained by multiplying and dividing the rotational constants for these 1-D rotors by a factor of 2). Uncertainties associated with our choices for the external rotational constants of the TS were also included. Upper limits to these values were obtained by setting them equal to those of the energized molecule, and lower limits were estimated by dividing the rotational constants used for the TS by a factor of 10.

Equation 1 explicitly includes the internal energy of the ion, E_i. All energy available is treated statistically, which should be a reasonable assumption because the internal energy of the reactants is redistributed throughout the ion upon impact with the collision gas. The threshold for dissociation is by definition the minimum energy required to lead to dissociation and thus corresponds to formation of products with no internal excitation.

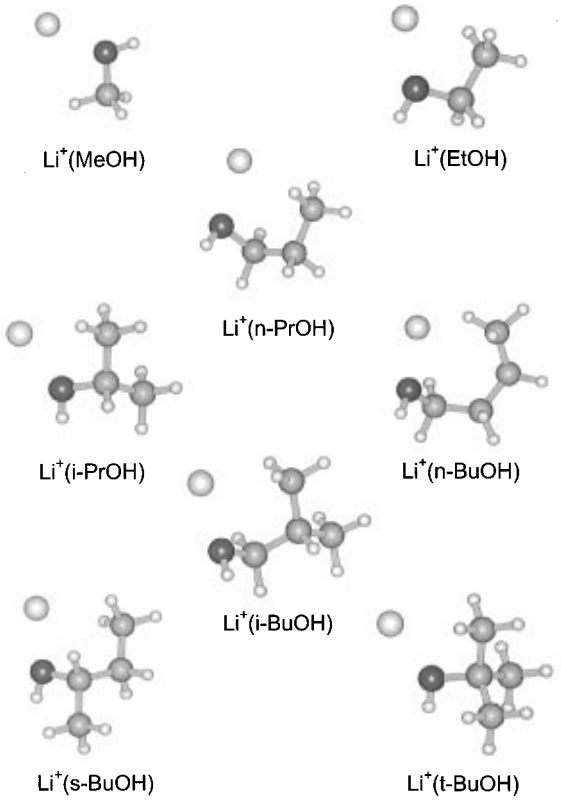

Figure 1. Semiempirical PM3-optimized geometries of Li^+(ROH) complexes, where ROH = methanol, ethanol, 1-propanol, 2-propanol, 1-butanol, 2-methyl-1-propanol, 2-butanol, and 2-methyl-2-propanol.

The assumption that products formed at threshold have an internal temperature of 0 K has been tested for several systems.[1,4,5,23] It has been shown that treating all energy of the ion (vibrational, rotational, and translational) as capable of coupling into the dissociation coordinate leads to reasonable thermochemistry. The threshold energies for dissociation reactions determined by analysis with eq 1 are converted to 0 K BDEs by assuming that E_0 represents the energy difference between reactants and products at 0 K.[40] This requires that there are no activation barriers in excess of the endothermicity of dissociation. This is generally true for ion−molecule reactions[38] and should be valid for the simple bond fission reactions examined here.[41]

Temperature Conversion. To compare bond energies measured here with enthalpies and free energies of dissociation determined in the literature, 0 K BDEs are converted to 298 and 373 K enthalpies and free energies using standard formulas.[42] The dissociation enthalpies for Li^+(ROH), ROH = methanol, ethanol, 1-propanol, 2-propanol, 1-butanol, 2-methyl-1-propanol, 2-butanol, and 2-methyl-2-propanol, at 298 K are obtained by adding 1.8, 2.0, 2.5, 2.1, 2.7, 2.3, 1.9, and 1.9 kJ/mol, respectively, to the 0 K BDEs. Similarly, dissociation enthalpies at 373 K are obtained by adding 1.6, 1.7, 2.3, 2.0, 2.5, 2.1, 1.7, and 1.6 kJ/mol, respectively, to the 0 K BDEs. The dissociation entropies of Li^+(ROH), ROH = methanol, ethanol, 1-propanol, 2-propanol, 1-butanol, 2-methyl-1-propanol, 2-butanol, and 2-methyl-2-propanol, at 298 K are 97.7, 97.7, 106, 101, 109, 106, 100, and 98.3 J/(K mol), respectively. Similarly, dissociation entropies at 373 K are 97.1, 97.1, 106, 100, 109, 105, 99.5, and 97.6 J/K mol, respectively.

Results

The geometry-optimized structures of the lithiated alcohols determined at the semiempirical PM3 level are shown in Figure 1. In all cases, the lithium ion prefers to be bound to the oxygen atom. The hydrocarbon backbone wraps around the lithium ion

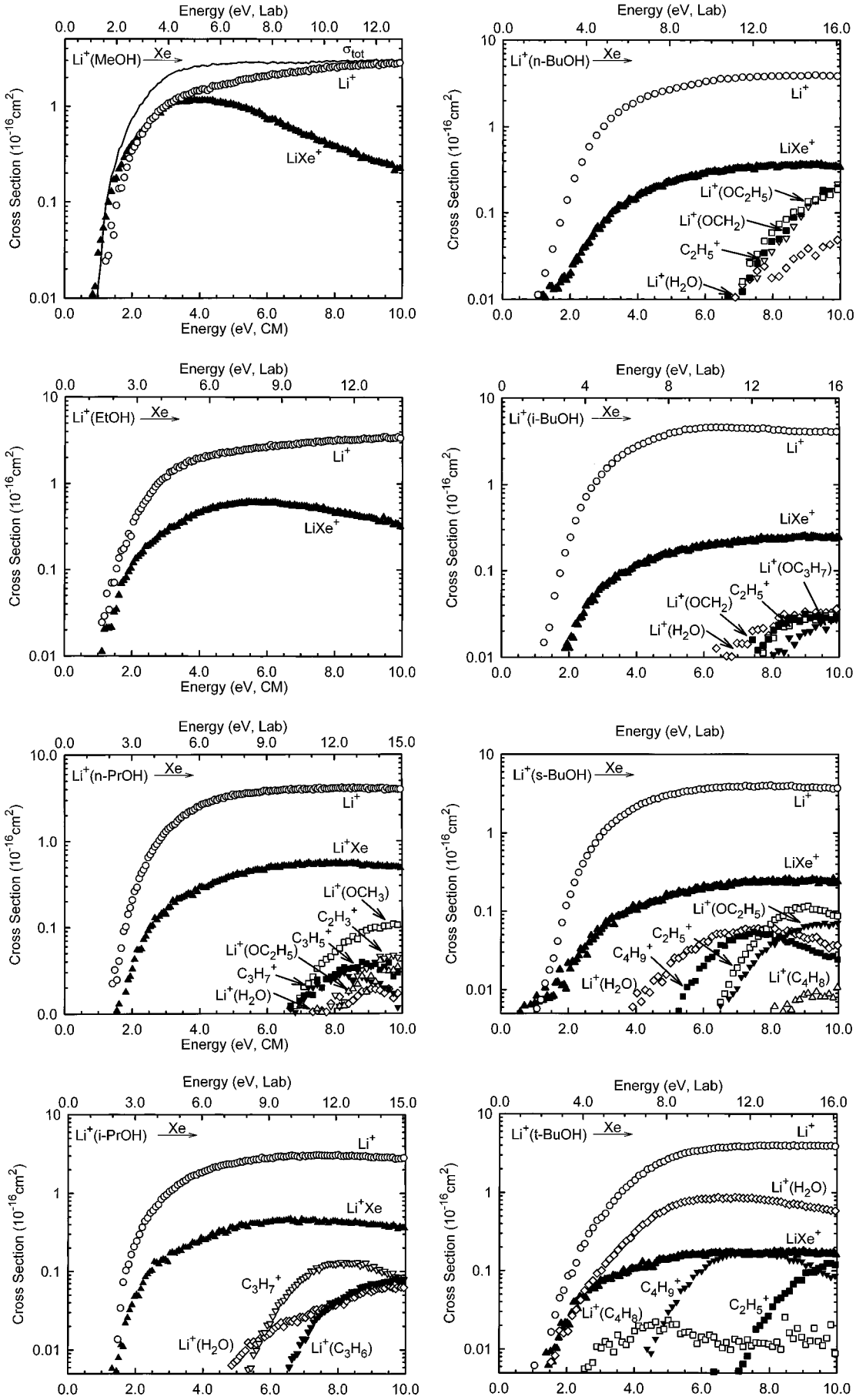

Figure 2. Cross sections for CID of Li^+(ROH), where ROH = methanol, ethanol, 1-propanol, 2-propanol, 1-butanol, 2-methyl-1-propanol, 2-butanol, and 2-methyl-2-propanol (parts a−h, respectively), as a function of kinetic energy in the center-of-mass frame (lower *x* axis) and the laboratory frame (upper *x* axis). Open circles show the cross sections for the primary product, Li^+. Filled triangles show the ligand exchange products, Li^+Xe. The remaining symbols show minor products resulting from high-energy bond cleavage reactions. In part a, the solid line shows the total cross section.

in such a way as to maximize the electrostatic interaction between the lithium ion and the alcohol while minimizing steric repulsion between the hydrogen atoms on neighboring sites. Other low-energy structures were also found in which the chelating effect was somewhat smaller, e.g., Li^+(*n*-BuOH) where only three carbons were wrapped around the Li ion. To verify that chelation is not an artifact of the parametrization used in the semiempirical calculations, *ab initio* calculations at the 6-31G** level were also performed on several of these complexes. The geometry-optimized structures were quite similar to those obtained at the semiempirical level. However, in these structures the chelating of the alcohol backbone was decreased slightly as a result of better alignment of the dipole moment of the alcohol with the Li^+-O bond. Because of our limited computational abilities, further *ab initio* calculations were not pursued, and semi-empirical results were used throughout for consistency. The Li^+ affinities calculated at the semiempirical level of theory are significantly lower than the experimentally determined values. This appears to be largely because Li^+ retains about 0.8−0.9 of its charge in its adducts,[43] whereas the PM3 calculations indicate that only 0.7−0.8 of the positive charge is retained by Li^+. The decreased charge retention by Li^+ in the calculated structures leads to longer Li^+-O bond distances, which ranged from 2.07 to 2.12 Å in the Li^+(ROH) complexes. For $Li^+(H_2O)$, PM3 calculations performed here yield a Li^+-O bond distance of 2.05 Å, while more sophisticated calculations give 1.85 Å.[44] Potentially, such discrepancies could influence the rotational constants used to model the data; however, the means used to estimate the uncertainties that result from these rotational constants already incorporate this 10% error in bond length.

Figure 2 shows experimental cross sections for the interaction of Xe with Li^+(ROH) complexes, where ROH = methanol, ethanol, 1-propanol, 2-propanol, 1-butanol, 2-methyl-1-propanol, 2-butanol, and 2-methyl-2-propanol. The primary (most favorable) process for all complexes is the loss of the intact alcohol in the collision-induced dissociation (CID) reaction 2.

$$Li^+(ROH) + Xe \rightarrow Li^+ + ROH + Xe \qquad (2)$$

As the size of the alcohol increases, the apparent threshold for reaction 2 increases from ~1 to 1.5 eV, consistent with an increase in the Li^+(ROH) bond energy that parallels the increase in the polarizability of the alcohols. The maximum cross section for this process is nearly constant increasing from 3 to 4 Å^2 as the size of the alcohol increases.

The cross sections for the ligand exchange reaction 3,

$$Li^+(ROH) + Xe \rightarrow Li^+Xe + ROH \qquad (3)$$

are large for methanol but decrease in importance as the size of the complexes increases. The maximum cross section for ligand exchange decreases from 1.2 to 0.25 Å^2 in going from methanol to 2-methyl-2-propanol. The apparent threshold for ligand exchange increases from 0.8 eV for methanol to 1.5 eV for 2-methyl-2-propanol. In the methanol system, the apparent threshold for ligand exchange is clearly below that for CID, consistent with the relative thermodynamics. As the alcohol gets larger, the apparent threshold for ligand exchange gradually shifts to higher energies relative to the CID process. This behavior reflects the reaction dynamics, as reaction 3 always has a lower thermodynamic threshold than reaction 2.

Products resulting from cleavage of the alcohol backbone are observed in the larger systems. Given the small size of these product cross sections and elevated energetics observed in the propanol systems, we did not attempt to collect similar products in the methanol and ethanol systems. For these dissociation pathways, the apparent thresholds decrease and the cross sections increase in going from a 1° to a 2° to a 3° alcohol. These products are very minor ($\sigma \leq 0.1$ Å^2) and occur at high energies (>5 eV) in all cases except the Li^+(*t*-BuOH) system. In this system, the largest of these products, $Li^+(H_2O)$, results from elimination of isobutene. Competing with this at low energies is the elimination of water to form the $Li^+(C_4H_8)$ complex. These two reactions, processes 4 and 5,

$$Li^+(ROH) + Xe \rightarrow Li(H_2O) + R-H + Xe \qquad (4)$$

$$Li^+(ROH) + Xe \rightarrow Li^+(R-H) + H_2O + Xe \qquad (5)$$

are also observed in the 2-propanol, 2-methyl-1-propanol, and 2-butanol systems (where the alcohol is branched), while only reaction 4 is observed in the 1-propanol and 1-butanol systems (where the alcohols are linear).

The other products observed in the 2-methyl-2-propanol system are alkyl ions, $C_4H_9^+$ and $C_2H_5^+$. The former product is formed in the reaction

$$Li^+(ROH) + Xe \rightarrow R^+ + LiOH + Xe \qquad (6)$$

Reaction 6 is also observed in all the propanol and butanol systems except 1-butanol. This product is not shown in the 2-methyl-1-propanol system as its maximum cross section is only 0.007 Å^2. This also indicates that our failure to observe this process in the 1-butanol system is probably due to its small size. Clearly, the prevalence and thresholds of these products are controlled by the relative ionization energies of the alkyl radicals,[45] 3° < 2° < 1°. The $C_2H_5^+$ product observed in the 2-methyl-2-propanol system is probably formed by decomposition of the primary $C_4H_9^+$ product.[46] Similarly, additional alkyl products observed in the other systems are likely to be formed by subsequent dissociation of the product of reaction 6. Indeed, the observation of a $C_2H_5^+$ product in the 1-butanol system provides evidence for reaction 6. Failure to observe the primary $C_4H_9^+$ product is reasonable because the cross sections for $C_2H_5^+$ have larger magnitudes than the $C_4H_9^+$ cross sections in the other three butanol systems.

All additional minor products observed correspond to reactions where a C−C bond is cleaved at elevated energies. In several systems, we observe loss of an alkyl radical from the initial complex, reaction 7.

$$Li^+(C_nH_{2n+1}OH) + Xe \rightarrow Li^+(C_{n-m}H_{2(n-m)}OH) + C_mH_{2m+1} + Xe \qquad (7)$$

In the 1-butanol and 2-methyl-1-propanol systems, we also observe $Li^+(CH_2O)$, although the mass is also consistent with $Li^+(C_2H_6)$. This process is believed to correspond to elimination of propane.

$$Li^+(C_4H_9OH) + Xe \rightarrow Li^+(CH_2O) + C_3H_8 + Xe \qquad (8)$$

Threshold Analysis. The model represented by eq 1 was used to analyze the thresholds for reaction 2 in all eight Li^+(ROH) systems. The results of these analyses are provided in Table 3. Figure 3 shows that the experimental cross sections for reaction 2 in all eight systems are accurately reproduced using a loose phase space limit (PSL) TS model. Good reproduction is obtained over energy ranges exceeding 2 eV and cross section magnitudes of at least a factor of 100. Table 3 includes three values of E_0: one that does not include the RRKM lifetime analysis and two where the lifetime analysis is included (a loose PSL and a tight TS model) as described above. The values obtained with no RRKM analysis should be very

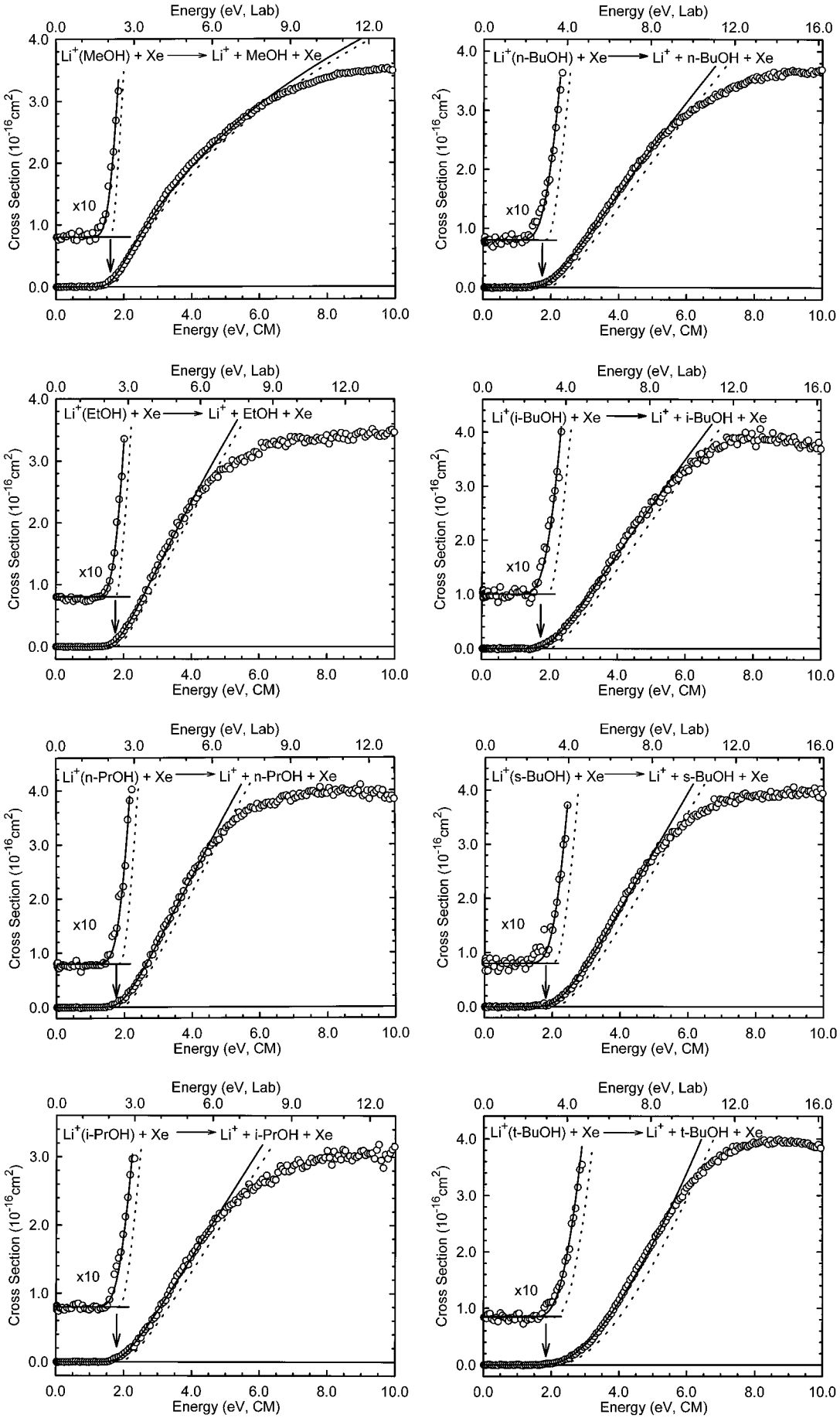

Figure 3. Cross sections for CID of $Li^+(ROH)$, where ROH = methanol, ethanol, 1-propanol, 2-propanol, 1-butanol, 2-methyl-1-propanol, 2-butanol, and 2-methyl-2-propanol (parts a−h, respectively), in the threshold region as a function of kinetic energy in the center-of-mass frame (lower *x* axis) and the laboratory frame (upper *x* axis). Open circles show the primary cross sections. The best fits to the data using the model of eq 1 convoluted over the neutral and ion kinetic and internal energy distributions are shown as solid lines. Dotted lines show the model cross sections in the absence of experimental kinetic energy broadening for reactants with an internal energy of 0 K. Average threshold energies are indicated by arrows.

TABLE 3: Bond Dissociation Energies at 0 K and Entropies of Activation at 1000 K of $Li^+(ROH)$[a]

alcohol	σ_0[b]	n[b]	E_0[c] (eV)	E_0 (PSL) (eV)	$\Delta S^\dagger$(PSL) (J/(mol K))	E_0(tight) (eV)	$\Delta S^\dagger$(tight) (J/(mol K))
MeOH	1.97 (0.31)	1.41 (0.05)	1.61 (0.09)	1.61 (0.09)	24 (21)	1.61 (0.09)	3
EtOH	1.94 (0.24)	1.73 (0.09)	1.71 (0.07)	1.69 (0.07)	35 (20)	1.59 (0.06)	−14
n-PrOH	2.18 (0.25)	1.77 (0.07)	1.84 (0.08)	1.77 (0.09)	45 (20)	1.56 (0.08)	−13
i-PrOH	1.45 (0.15)	1.74 (0.06)	1.88 (0.08)	1.79 (0.08)	42 (20)	1.58 (0.07)	−15
n-BuOH	1.59 (0.14)	1.71 (0.05)	1.92 (0.08)	1.75 (0.08)	49 (21)	1.47 (0.08)	−13
i-BuOH	0.99 (0.05)	1.72 (0.03)	1.95 (0.07)	1.75 (0.08)	46 (20)	1.48 (0.08)	−14
s-BuOH	1.82 (0.15)	1.82 (0.05)	2.04 (0.08)	1.81 (0.09)	41 (20)	1.54 (0.09)	−13
t-BuOH	0.67 (0.12)	2.27 (0.10)	2.14 (0.10)	1.85 (0.11)	39 (20)	1.58 (0.10)	−14

[a] Uncertainties are listed in parentheses. [b] Average values for loose PSL transition state. [c] No RRKM analysis.

conservative upper limits to the true thermodynamic thresholds, while those obtained with a tight TS provide very conservative lower limits. The best values are expected to arise from the loose TS model, an assumption that has been tested in several systems previously.[2,3,10,47] Although the PSL treatment for loose TSs used here differs somewhat from our previous methodology, empirically the threshold results for loose TSs determined here and with our previous methods are found to be very similar.[17] The present system provides a good test of the accuracy of the loose PSL TS model because our results can be compared with those of Taft et al.;[7] see below.

Comparison of the three E_0 values in Table 3 shows that the kinetic shifts vary with the size and geometry of the alcohol. Dissociation of Li^+(MeOH) shows no kinetic shift (even when a tight TS is used). As the size of the alcohol increases, the kinetic shift gradually increases reaching a maximum for Li^+-(*t*-BuOH), which exhibits a kinetic shift of approximately 0.29 eV when determined with a loose PSL TS and 0.56 eV when determined with a tight TS. This is reasonable because the Li^+-(MeOH) system has only three heavy atoms and 15 vibrational modes while the butanol systems have six heavy atoms and 42 vibrational modes. Kinetic shifts vary among the butanol systems (0.17 eV for 1-butanol to 0.29 eV for 2-methyl-2-propanol) because they couple with the dissociation energy (higher E_0 values lead to larger kinetic shifts) and TS geometries. The latter are reflected by the entropies of activation, $\Delta S^\dagger$, a measure of the tightness or looseness of the TS. Listed in Table 3 at 1000 K, the $\Delta S^\dagger$(PSL) values can be seen to increase from the methanol to the ethanol to the propanol to the 1-butanol systems and then decrease somewhat as the butanols become more compact. These entropies of activation can be favorably compared to $\Delta S^\dagger_{1000}$ values in the range 29−46 J/(K mol) collected by Lifshitz for several simple bond cleavage dissociations of ions.[48] Considering that the TS is expected to lie at the centrifugal barrier for association of Li^+ + ROH, the negative entropies of activation obtained for the tight TS clearly indicate that this model provides a very conservative limit for the kinetic shift.

Thresholds of Minor Products. Analysis of the energy dependence of the cross sections for minor products is difficult because of the strong competition of these channels with the much more efficient CID channel to yield Li^+ + ROH. For all but the 2-methyl-2-propanol system, these reaction channels are strongly disfavored energetically. Analysis of the cross sections for reactions 4 and 5 is further complicated by the fact that the transition states for these channels do not correspond to loose associations of the final products but to a tight TS linking the Li^+(ROH) and $(H_2O)Li^+$(R−H) intermediates, as shown for the example of *t*-BuOH in Figure 4. Hence, we analyze the thresholds for these two channels relative to that for Li^+ using eq 1 with no RRKM lifetime effects included. In the case of *t*-BuOH, we were struck by the very similar shapes of the Li^+ and $Li^+(H_2O)$ cross sections in the threshold region. Hence, our analysis included holding the parameter n constant at 2.3 (as listed in Table 3) for the $Li^+(H_2O)$ channel, as well as

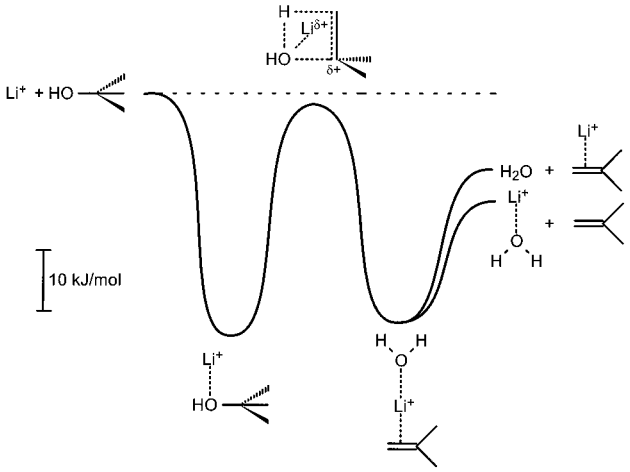

Figure 4. Schematic representation of the potential surface at 0 K for the Li^+ induced dehydration reaction of 2-methyl-2-propanol. Thermochemistry for the Li^+(2-methyl-2-propanol) intermediate and transition state are taken from the present study. The $Li^+(H_2O)$ bond energy is taken from DK (ref 9), and the relative bond energy of $Li^+(C_4H_8)$ is from Staley and Beauchamp (ref 11). $D(C_4H_8Li^+-OH_2)$ is assumed to equal $D(H_2OLi^+-OH_2)$ taken from ref 10.

allowing this parameter to vary freely (optimized value of n = 2.4). These procedures give average thresholds for the Li^+ and $Li^+(H_2O)$ channels of 2.14 ± 0.10 (Table 3) and 2.00 ± 0.14 eV, respectively. The $Li^+(C_4H_8)$ channel was sufficiently small that it could not be fit reliably. However, the threshold region of this channel can be reproduced well by holding E_0 fixed at 2.0 eV and allowing σ_0 and n to vary. This led to a decrease in n to ∼1.4. The very different values of n needed to reproduce these cross sections is not unexpected as evidenced by the strong energy dependence observed in the branching ratio between these two minor products, as discussed further below. Thus, the thresholds for the two reactive channels are found to equal one another within experimental error and to differ from the energy of the Li^+ + *t*-BuOH asymptote by 0.14 ± 0.17 eV.

Similar analyses of the thresholds of the $Li^+(H_2O)$ and R^+ product cross sections were performed for the other alcohol systems. Thresholds energies (uncorrected for lifetime affects) of 4.2 ± 0.6, 3.0 ± 0.6, 5.6 ± 1.3, 3.5 ± 0.5, and 3.0 ± 0.5 eV are obtained for formation of $Li^+(H_2O)$ in the 1-propanol, 2-propanol, 1-butanol, 2-methyl-1-propanol, and 2-butanol systems, respectively. These values lie 2.3 ± 0.6, 1.1 ± 0.6, 3.7 ± 1.3, 1.6 ± 0.5, and 1.0 ± 0.5 eV above the respective thresholds for the Li^+ + ROH products. In all cases, the thresholds obtained have large uncertainties because the cross sections rise so slowly with energy, a consequence of the high thresholds, tight transition state, and competition with the CID channel. Because of this behavior, it is likely that the thresholds are upper limits to the true thresholds for these reactions. Threshold energies for formation of R^+ in the 2-propanol, 2-butanol, and 2-methyl-2-propanol systems yielded thresholds (uncorrected for lifetime effects) of 5.1 ± 0.2, 4.5 ± 0.4, and 4.1 ± 0.4 eV, respectively. These values lie an average of 1.5

TABLE 4: Enthalpies and Free Energies of Lithium Ion Binding of ROH at 373 K in kJ/mol[a]

alcohol	ΔH_0	$\Delta H_{373} - \Delta H_0$	$T\Delta S_{373}$	ΔG_{373}	ΔG_{373}[b]
ammonia		4.5 (0.8)	36.4 (1.6)		138.1 (8.4)
water		4.4 (0.4)	35.5 (0.7)		114.2 (8.4)
MeOH	155.0 (8.5)	1.6 (0.6)	36.2 (2.1)	120.4 (8.8)	130.5 (8.4)
EtOH	163.5 (6.5)	1.7 (0.7)	36.2 (2.1)	129.0 (6.9)	138.5 (8.4)
n-PrOH	170.3 (8.6)	2.3 (0.8)	39.4 (2.1)	133.2 (8.9)	142.7 (8.4)
i-PrOH	172.8 (7.5)	2.0 (0.7)	37.3 (2.0)	137.5 (7.8)	146.4 (8.4)
n-BuOH	168.6 (8.2)	2.6 (0.9)	40.5 (2.1)	130.7 (8.5)	150.0 (8.4)
i-BuOH	168.8 (7.6)	2.1 (0.8)	39.2 (2.1)	131.7 (7.9)	147.3 (8.4)
s-BuOH	174.3 (8.9)	1.7 (0.6)	37.1 (2.1)	138.9 (9.2)	150.2 (8.4)
t-BuOH	178.2 (10.2)	1.6 (0.7)	36.4 (2.1)	143.4 (10.4)	

[a] Uncertainties are listed in parentheses. [b] Measured in ref 6. These values should be lowered by 7.1−13.4 kJ/mol; see discussion in text.

TABLE 5: Enthalpies and Free Energies of Lithium Ion Binding and Proton Affinities of ROH at 298 K in kJ/mol[a]

alcohol	ΔH_0	$\Delta H_{298} - \Delta H_0$	ΔH_{298}	$T\Delta S_{298}$	ΔG_{298}	ΔG_{298}[b]	PA_{298}[c]
ammonia		4.3 (0.7)		28.9 (1.1)		134.3 (8.4)	
water		4.1 (0.3)		28.2 (0.5)		114.1 (8.4)	
MeOH	155.0 (8.5)	1.8 (0.5)	156.8 (8.5)	29.1 (1.5)	127.7 (8.6)	126.8 (8.4)	761.1
EtOH	163.5 (6.5)	2.0 (0.6)	165.5 (6.5)	29.1 (1.6)	136.4 (6.7)		787.8
n-PrOH	170.3 (8.6)	2.5 (0.7)	172.8 (8.6)	31.7 (1.8)	141.1 (8.8)		798.3
i-PrOH	172.8 (7.5)	2.1 (0.6)	174.9 (7.5)	30.0 (1.5)	144.9 (7.7)		800.0
n-BuOH	168.6 (8.2)	2.7 (0.7)	171.3 (8.2)	32.6 (1.5)	138.7 (8.4)		799.6
i-BuOH	168.8 (7.6)	2.3 (0.7)	171.1 (7.6)	31.5 (1.6)	139.6 (7.8)		800.0
s-BuOH	174.3 (8.9)	1.9 (0.6)	176.2 (8.9)	29.9 (1.6)	146.3 (9.1)		810.5
t-BuOH	178.2 (10.2)	1.9 (0.6)	180.1 (10.2)	29.3 (1.6)	150.8 (10.3)		810.4

[a] Uncertainties are listed in parentheses. [b] Taken from ref 11. [c] Taken from ref 44.

± 0.5 eV above the thermodynamic thresholds. Considering the high threshold energies involved, most of this shift could easily be due to lifetime effects. A more detailed analysis of the cross sections for these and other minor channels was not pursued because the problems noted above led us to conclude such an analysis was unlikely to provide reliable thermochemistry.

Discussion

Lithium Ion Binding Affinities. To compare the thermochemistry obtained here with the literature values of Taft et al.,[7] we convert our values to free energies of dissociation at 373 K. (There is some ambiguity about the appropriate temperature for these ICR studies. No details regarding the determination of the 373 K temperature are provided in the paper of Taft et al. In contrast, Woodin and Beauchamp (WB),[12] who performed similar experiments on a similar apparatus report their values at 298 K and mention that the filament used to supply Li^+ raised the temperature of the ICR cell by less than 5 deg.) Our experimental results (determined with threshold analyses corrected for lifetime effects assuming a loose PSL TS) at 0 K, ΔH_0, are listed in Table 4 along with the enthalpy differences and entropies needed to convert to ΔG_{373} values. The final ΔG_{373} values for Li^+(ROH) are listed along with those measured by Taft et al. in Table 4. (A similar conversion to 298 K values is presented in Table 5.) The ΔG_{373} values of Taft et al. are systematically higher than our values by an average of 12 ± 4 kJ/mol. Although this discrepancy is within the combined experimental errors of the two techniques, the agreement is not very satisfying.

As noted in the Introduction, the values of Taft et al.[7] are anchored to an absolute Li^+ affinity scale by adjusting the ΔG for dissociation of $Li^+(NH_3)$ measured by WB[12] from 298 to 373 K. The correction made by Taft et al. is obviously wrong because the free energy for dissociation at 373 K should be *lower* than that at 298 K, while the 373 K value cited by Taft et al. for Li^+-NH_3 is *higher* than the free energy of dissociation obtained from WB at 298 K. A direct comparison of our results for methanol converted to ΔG_{298} with those of WB shows excellent agreement (Table 5), as does a previous result for the binding of Li^+ with dimethyl ether.[2] If we reconstruct the calibration of Taft et al., we find that the $\Delta G_{298}(Li^+-NH_3)$ value reported by WB should correspond to a ΔG_{373} value of 127.0 kJ/mol rather than the 138.1 kJ/mol value cited by Taft et al. Alternatively, we could start with the value of Dzidic and Kebarle (DK) for $\Delta H_{298}(Li^+-H_2O)$ and convert this to $\Delta G_{298}(Li^+-H_2O)$ (Table 5) and to $\Delta G_{373}(Li^+-H_2O)$ (Table 4). This latter value is 107.1 kJ/mol compared to the value of 114.2 kJ/mol cited by Taft et al. Likewise, WB's values for methanol and dimethyl ether translate to $\Delta G_{373}(Li^+-MeOH) = 119.5$ kJ/mol and $\Delta G_{373}(Li^+-Me_2O) = 122.2$ kJ/mol, in contrast to 130.5 and 135.1 kJ/mol reported by Taft et al. Overall, the values of Taft et al. differ from WB's values by 11.1, 7.1, 11.0, and 12.9 kJ/mol for these three systems (NH_3, H_2O, MeOH, and Me_2O), nearly equal to the 12 ± 4 discrepancy noted above. In addition, comparison of the six other systems studied by WB reveal comparable differences of between 8.1 and 13.4 kJ/mol (average deviation for these six systems of 10.4 ± 2.3 kJ/mol). Apparently, Taft et al. made an arithmetic error in the conversion of WB's data to the temperature appropriate for their experimental study. Thus, a proper comparison of their results and ours requires that their values be adjusted first by decreasing between 7.1 and 13.4 kJ/mol. (Further, it seems likely that the adjustment should be toward the high end of this range because the differences between the values of Taft et al. and properly adjusted values from WB for systems with Li^+ affinities comparable to the alcohols average 12 ± 1 kJ/mol.) This comparison is shown in Figure 5. The agreement between the adjusted values of Taft et al. and the present results is excellent in all but two cases: 1-butanol and 2-methyl-1-propanol. With an adjustment of 12 ± 1 kJ/mol, these two cases have remaining discrepancies of 7.3 and 3.6 ± 1 kJ/mol, well within the experimental uncertainty of either measurement. The trends in the ΔG_{373} values observed here can be rationalized fairly easily. We first note that the three larger primary alcohols (1-propanol, 1-butanol, and 2-methyl-1-propanol) have similar free energies of binding: 133.2, 130.7, and 131.7 kJ/mol, respectively. The free energies of binding for the secondary alcohols (2-propanol and 2-butanol) are also similar, 137.5 and 138.9 kJ/mol, respectively, and larger than those for the primary alcohols.

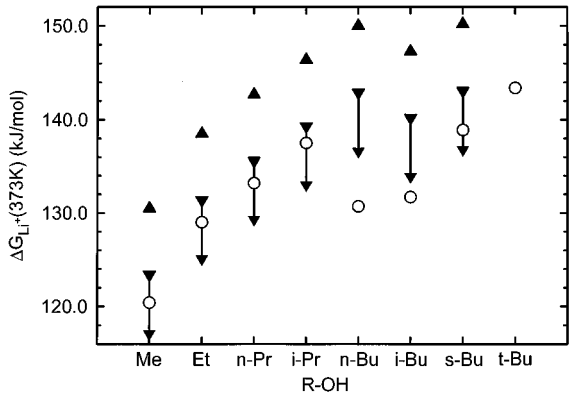

Figure 5. Free energy of Li^+ binding of various alcohols at 373 K in kJ/mol. Open circles show present CID results. Closed triangles show results from equilibrium ICR measurements (ref 7). Inverted triangles show the range of values spanned after correcting the ICR values by 7.1−13.4 kJ/mol as discussed in the text.

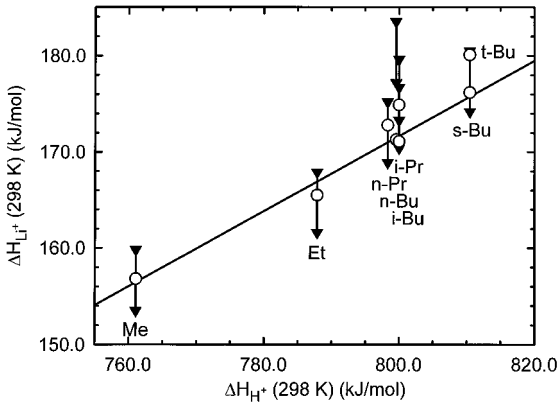

Figure 6. Li^+ binding affinities vs proton affinities at 298 K (in kJ/mol) of Li^+−(ROH), where ROH = methanol, ethanol, 1-propanol, 2-propanol, 1-butanol, 2-methyl-1-propanol, 2-butanol, and 2-methyl-2-propanol. Proton affinities are taken from ref 45.

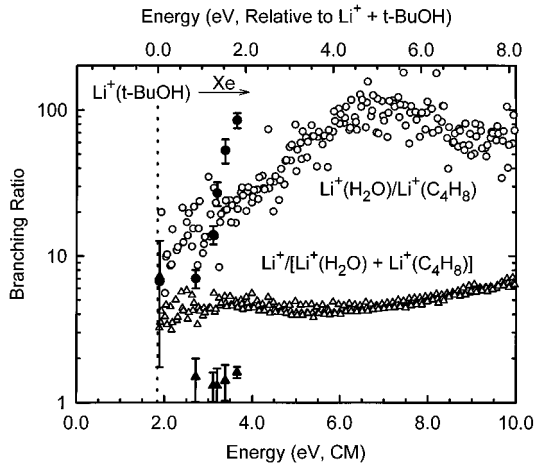

Figure 7. Branching ratios for CID of Li^+(t-BuOH) as a function of kinetic energy in the center-of-mass frame (lower *x* axis) and relative to the energy of Li^+ + *t*-BuOH (upper *x* axis). Open circles show the branching ratios for $Li^+(H_2O)$ vs $Li^+(C_4H_8)$ from multiple data sets. Open triangles show the branching ratios for Li^+ vs $[Li^+(H_2O) + Li^+(C_4H_8)]$ from multiple data sets. Closed symbols show analogous data taken from refs 49 (lowest energy point) and 50 (higher energy points).

Finally, 2-methyl-2-propanol, the lone tertiary alcohol, has an even greater free energy of binding, 143.4 kJ/mol. Thus, the ΔG_{373} values increase by 5−6 kJ/mol as one progresses from primary to secondary and secondary to tertiary alcohols. In contrast, Taft et al. observe that the free energies of binding depend more critically on the number of carbon atoms.

Overall, it seems that the loose PSL analysis of the CID cross sections is providing accurate relative and absolute numbers. In this regard, it is worth noting that each CID measurement is a completely independent determination of an absolute bond energy. Although systematic errors for a series of systems such as the Li^+(alcohol) complexes are likely to be similar, the relative bond energies may not be as precisely determined as in equilibrium measurements. The errors listed with these bond enthalpies and free energies (Tables 4 and 5) reflect the uncertainties in determining the threshold energies given that the PSL model correctly estimates the kinetic shift. The comparison with the literature data makes it clear that neither the no RRKM nor the tight TS models yield accurate relative or absolute bond energies for the Li^+(alcohol) complexes. Hence, it is inappropriate to use either of these models to provide much more conservative error bars for the loose PSL model values.

Another means of assessing how reasonable the trends in the present results are is to compare the lithium ion affinities of the alcohols with their proton affinities (PAs). Our experimental results for $\Delta H_{298}(Li^+-ROH)$, ROH = methanol, ethanol, 1-propanol, 2-propanol, 1-butanol, 2-methyl-1-propanol, 2-butanol, and 2-methyl-2-propanol, are compared with enthalpies of H^+ binding at 298 K in Table 5 and Figure 6. A linear correlation between the lithium ion affinity and the proton affinity is found. Further, we note that the PAs of 1-butanol and 2-methyl-1-propanol are very similar to that of 1-propanol, a result similar to that obtained here for the Li^+ affinities. In contrast, the corrected Li^+ affinity values for 1-butanol and 2-methyl-1-propanol from Taft et al. lie substantially higher than that for 1-propanol. It may be significant that the Li^+ affinities for 2-methyl-2-propanol and 2-propanol lie above the overall correlation with PA, which is largely determined by values for primary alcohols. This may indicate enhanced stability of the Li^+(ROH) species due to contributions from the LiOH−R^+ resonance structure.

Minor Products: Dehydration Reactions. The minor products observed in the CID reactions should correlate with products observed in bimolecular reactions of Li^+ with ROH. The most extensive work along these lines is that by Allison and Ridge (AR),[49] who found that 2-propanol, 1-butanol, and 2-methyl-1-propanol did not react with Li^+ at thermal energies in an ion cyclotron resonance (ICR) mass spectrometer. The products of reactions 4 and 5 were observed only for the case of 2-methyl-2-propanol. This result was examined in depth by Creasy and Farrar (CF) using crossed beams methodology in a pair of papers.[50]

The observations of AR agree with the present study which finds that the minor products appear at energies well in excess of the threshold for production of Li^+ + ROH except in the case of 2-methyl-2-propanol. In this system, both the $Li^+(H_2O)$ and $Li^+(C_4H_8)$ products have thresholds very close to that of Li^+ (although this is not obvious in Figure 2h for the $Li^+(C_4H_8)$ product because of the logarithmic scale used). AR do not report a rate constant for the Li^+ + 2-methyl-2-propanol system but do mention that the reactions observed have rate constants between 2 and 10×10^{-10} cm^3/s. This corresponds to a reaction efficiency (compared to the Langevin-Gioumousis-Stevenson collision limit[51] of 2.7×10^{-9} cm^3/s) of 7−37%. CF report nonreactive to reactive branching ratios that start from 1.5 ± 0.5 at 0.85 eV, dip to 1.3 ± 0.3 at about 1.3 eV, and then increase to 1.6 ± 0.1 at 1.8 eV, where the energies are relative to the Li^+ + *t*-BuOH reactants. These results are shown in Figure 7. Thus, the branching ratios are relatively constant and correspond to reaction efficiencies between 33 and 50%. The ratio of our Li^+ cross section to that for the sum of the $Li^+(H_2O)$ and $Li^+(C_4H_8)$ cross sections in the threshold region (1.85 eV relative to the Li^+(t-BuOH) intermediate and approximately

zero relative to $Li^+ + t$-BuOH) is 4.3 ± 0.9 (Figure 7). Thus, the comparable reaction efficiency (reactive/total cross sections) is 19 ± 3%. Although this reaction efficiency is somewhat lower than the values of CR, the agreement is reasonable considering the very different methods used. Also, the branching ratio of nonreactive to reactive scattering is likely to be influenced by the excitation method; i.e., Li^+(*t*-BuOH) complexes formed in bimolecular collisions have very different internal and angular momentum distributions compared with these complexes excited by a collision with Xe.

The most notable observation concerning the reaction efficiency is that our results find it invariant from threshold to about 8 eV, a 6 eV range of energies (Figure 7). CR also commented on this invariance although their results (also shown in Figure 7) covered a much smaller range of energies, 1 eV. It is straightforward to see that this means the threshold energies for the Li^+ and $Li^+(H_2O)$ and, less obviously, the $Li^+(C_4H_8)$ products are virtually the same. CR reached the same conclusion based on a phase space analysis of the branching ratios. Here, we can also assess more quantitatively by analyzing the energy dependence of the cross sections for $Li^+(H_2O)$ and $Li^+(C_4H_8)$. As described above, this analysis did not include lifetime effects because of the tight transition state associated with the dehydration reactions (Figure 4). Relative thresholds for the two dehydration reaction channels are found to equal one another within experimental error and to lie below the energy of the $Li^+ + t$-BuOH asymptote by only 0.14 ± 0.17 eV. This value agrees well with the value of 0.00 ± 0.05 eV determined by CR. These energetics are indicated in Figure 4.

AR report a branching ratio between reactions 4 and 5 as 6.7 at thermal energies, while CR found that this ratio increased from 7 ± 1 at 0.85 eV to almost 100 at 1.8 eV where the energies are relative to $Li^+ + t$-BuOH. We find a ratio close to 10 at threshold (~0 eV relative to $Li^+ + t$-BuOH), increasing to about 100 ± 30 by 6.5 eV (4.65 eV relative to $Li^+ + t$-BuOH), and then decreasing to 60 ± 20 by 10 eV (8.15 eV relative to $Li^+ + t$-BuOH). Thus, the qualitative behavior is similar to that observed by CR except that the large increase in branching ratio is spread over a larger energy range. This simply reflects the fact that, in a bimolecular reaction of $Li^+ + t$-BuOH, all of the collision energy is retained by the transient Li^+(*t*-BuOH) complex, while in a collision-induced process, the Li^+(t-BuOH) complex has a range of internal energies extending from the center-of-mass frame collision energy down to zero. Hence, the average energy deposited in the complex is some fraction of the collision energy. Comparisons of the energies where the branching ratio reaches 100 in the two studies (1.8 eV by CR and 4.65 eV above the threshold for $Li^+ + t$-BuOH in the present work) suggest that this fraction is about 40% in this system. This can be compared with an estimate of 21% calculated for impulsive collisions.[52]

For the other alcohols, we observe that thresholds for production of $Li^+(H_2O)$ lie above those for Li^+ by 0.4−1.7 eV for the secondary alcohols and by 1.1−4.9 eV for the primary alcohols. These values track roughly with the ionization energies (IEs) of the alkyl fragments, i.e., the IEs of the secondary alkyls lie approximately 0.6 ± 0.1 eV above that for *tert*-butyl, and the primary alkyls have IEs that are about 1.3 ± 0.1 eV higher than IE(*tert*-butyl).[45] This trend makes sense based on the character expected for the transition state connecting the Li^+(ROH) and $(H_2O)Li^+$(R−H) intermediates, as discussed more fully in the next section.

Minor Products: LiOH + R^+ Formation. In their study of the reactions of alkali ions with many alcohols and alkyl halides, AR noted that the reactivity increases as the alkyl varies from primary to secondary to tertiary. This trend is also obvious in the present data. The thresholds for the minor products are lowest for 2-methyl-2-propanol, intermediate for 2-propanol and 2-butanol, and highest (>6 eV) for the primary alcohols 1-propanol, 1-butanol, and 2-methyl-1-propanol. On the basis of this trend, AR suggested that the rearrangement between the Li^+(ROH) and the $(H_2O)Li^+$(R−H) intermediates had character like $(LiOH)R^+$, which we have indicated by the partial charges for this transition state in Figure 4. The observation of reaction 6 provides some direct experimental evidence of the importance of such character as does the correlation noted above between IE(R) values and the thresholds measured for the $Li^+(H_2O)$ products. In the 2-methyl-2-propanol system, the formation of $C_4H_9^+$ is prominent at elevated energies. Further, the $Li^+(C_4H_8)$ cross section peaks near the threshold for the alkyl ion product, showing evidence of competition between these two products. Such competition is not obvious for the $Li^+(H_2O)$ cross section primarily because of its much larger magnitude. Likewise, in the two secondary alcohol systems, the R^+ products are prominent. For the primary alcohols, the alkyl ions are not observed until much higher in energy, consistent with the much higher ionization energies of primary alkyls.

Minor Products: C−C Bond Cleavage. The other class of minor ionic products correspond to chemical formulae of $Li^+(OCH_2)$ and $Li^+(OC_nH_{2n+1})$. The former product is observed for the 1-butanol and 2-methyl-1-propanol systems and presumably is formed by a 1,3-hydrogen shift from oxygen, followed by cleavage of the $C_\alpha-C_\beta$ bond, thereby eliminating propane. The latter products could have alkoxy structures, also formed by a 1,3-hydrogen shift from oxygen, followed by cleavage of the $C_\beta-C_\gamma$ bond. Another possibility at the elevated energies where the $Li^+(OC_nH_{2n+1})$ products are observed is that they are the result of simple C−C bond cleavage reactions that form $Li^+(HOC_nH_{2n})$ complexes, which could then rearrange to more stable structures. It is interesting that these C−C bond cleavage products are not as important in the tertiary and secondary alcohol systems (Figure 2d,g,h), presumably because cleavage at the O−R bond is more facile.

Conclusions

The kinetic energy dependences of the collision-induced dissociations of Li^+(ROH), ROH = methanol, ethanol, 1-propanol, 2-propanol, 1-butanol, 2-methyl-1-propanol, 2-butanol, and 2-methyl-2-propanol, with Xe are examined in a guided ion beam mass spectrometer. The dominant dissociation process in all cases is formation of $Li^+ + ROH$. Thresholds for these processes are determined after consideration of the effects of reactant internal energy, multiple collisions with Xe, and lifetime effects (using a newly revised methodology described in detail elsewhere).[17] These thresholds are converted to enthalpies and free energies at 298 and 373 K for comparison with previous equilibrium data on these systems. It is found that our results agree well with those of Woodin and Beauchamp[12] for the methanol system but that results of Taft et al.[7] are flawed by incorrect adjustments for differing experimental temperatures. Once these latter values are correctly revised, the agreement with the present results is excellent for five of seven alcohols jointly studied and within experimental error for the other two alcohols.

In the larger alcohol systems, collisional activation of Li^+(ROH) with Xe also yields minor products corresponding to dehydration reactions, formation of $LiOH + R^+$, and simple C−C cleavage reactions. In the 2-methyl-2-propanol system, these results are favorably compared with those observed in the bimolecular reaction of Li^+ with 2-methyl-2-propanol by Allison and Ridge[49] and Creasy and Farrar.[50] In this system, we determine that the barrier to rearrangement of the Li^+(*t*-

BuOH) intermediate lies 0.14 ± 0.17 eV below the energy of the Li^+ + *t*-BuOH asymptote. Further, we find evidence for the importance of $(LiOH)R^+$ intermediates as proposed by AR.

Acknowledgment. Funding for this work was provided by the National Science Foundation under Grant CHE-9530412 and partial funding by the donors of the Petroleum Research Fund, administered by the American Chemical Society.

References and Notes

(1) Khan, F. A.; Clemmer, D. C.; Schultz, R. H.; Armentrout, P. B. *J. Phys. Chem.* **1993**, *97*, 7978.
(2) More, M. B.; Glendening, E. D.; Ray, D.; Feller, D.; Armentrout, P. B. *J. Phys. Chem.* **1996**, *100*, 1605.
(3) Ray, D.; Feller, D.; More, M. B.; Glendening, E. D.; Armentrout, P. B. *J. Phys. Chem.* **1996**, *100*, 16116.
(4) Dalleska, N. F.; Honma, K.; Armentrout, P. B. *J. Am. Chem. Soc.* **1993**, *115*, 12125.
(5) Dalleska, N. F.; Honma, K.; Sunderlin, L. S.; Armentrout, P. B. *J. Am. Chem. Soc.* **1994**, *116*, 3519.
(6) Chupka, W. A. *J. Chem. Phys.* **1959**, *30*, 191.
(7) Taft, R. W.; Anvia, F.; Gal, J.-F.; Walsh, S.; Capon, M.; Holmes, M. C.; Hosn, K.; Oloumi, G.; Vasanwala, R.; Yazdani, S. *Pure Appl. Chem.* **1990**, *62*, 17.
(8) McLuckey, S. A.; Cameron, D.; Cooks, R. G. *J. Am. Chem. Soc.* **1981**, *103*, 1313.
(9) Dzidic, I.; Kebarle, P. *J. Phys. Chem.* **1970**, *74*, 1466.
(10) Rodgers, M. T.; Armentrout, P. B. *J. Phys. Chem.*, in press.
(11) Staley, R. H.; Beauchamp, J. L. *J. Am. Chem. Soc.* **1975**, *97*, 5920.
(12) Woodin, R. L.; Beauchamp, J. L. *J. Am. Chem. Soc.* **1978**, *100*, 501.
(13) Bojesen, G.; Breindahl, T.; Andersen, U. *Org. Mass Spectrom.* **1993**, *28*, 1448.
(14) Cerda, B. A.; Wesdemiotis, C. submitted *J. Am. Chem. Soc.* **1996**, *118*, 11884.
(15) Walter, D.; Armentrout, P. B. Submitted for publication.
(16) Rodgers, M. T.; Armentrout, P. B. Work in progress.
(17) Rodgers, M. T.; Ervin, K. M.; Armentrout, P. B. *J. Chem. Phys.*, in press.
(18) Ervin, K. M.; Armentrout, P. B. *J. Chem. Phys.* **1985**, *83*, 166.
(19) Schultz, R. H.; Armentrout, P. B. *Int. J. Mass Spectrom. Ion Processes* **1991**, *107*, 29.
(20) Teloy, E.; Gerlich, D. *Chem. Phys.* **1974**, *4*, 417. Gerlich, D. Diplomarbeit, University of Freiburg, Federal Republic of Germany, 1971. Gerlich, D. In *State-Selected and State-to-State Ion-Molecule Reaction Dynamics, Part I, Experiment*; Ng, C.-Y., Baer, M., Eds.; *Adv. Chem. Phys.* **1992**, *82*, 1.
(21) Aristov, N.; Armentrout, P. B. *J. Phys. Chem.* **1986**, *90*, 5135.
(22) Hales, D. A.; Armentrout, P. B. *J. Cluster Sci.* **1990**, *1*, 127.
(23) Schultz, R. H.; Crellin, K. C.; Armentrout, P. B. *J. Am. Chem. Soc.* **1992**, *113*, 8590.
(24) Schultz, R. H.; Armentrout, P. B. *J. Chem. Phys.* **1992**, *96*, 1046.
(25) Fisher, E. R.; Kickel. B. L.; Armentrout, P. B. *J. Phys. Chem.* **1993**, *97*, 10204.
(26) Fisher, E. R.; Kickel, B. L.; Armentrout, P. B. *J. Chem. Phys.* **1992**, *97*, 4859.
(27) Hyperchem Computational Chemistry Software Package, Version 4.5, Hypercube Inc., 1996.
(28) Stewart, J. J. P. *J. Comput. Chem.* **1989**, *10*, 209.
(29) Stewart, J. J. P. *J. Comput. Chem.* **1989**, *10*, 221.
(30) Anders, E.; Koch, R.; Freunscht, P. *J. Comput. Chem.* **1993**, *14*, 1301.
(31) Seeger, D. M.; Korzeniewski, C.; Kowalchyk, W. *J. Phys. Chem.* **1991**, *95*, 6871.
(32) Fogarasi, G.; Pulay, P. In *Vibrational Spectra and Structure*; Durig, J. R., Ed.; Elsevier: New York, 1985; Vol. 14, p 125.
(33) Beyer, T. S.; Swinehart, D. F. *Commun. ACM* **1973**, *16*, 379. Stein, S. E.; Rabinovitch, B. S. *J. Chem. Phys.* **1973**, *58*, 2438. Stein, S. E.; Rabinovitch, B. S. *Chem. Phys. Lett.* **1977**, *49*, 1883.
(34) Gilbert, R. G.; Smith, S. C. *Theory of Unimolecular and Recombination Reactions*; Blackwell Scientific Publications: Oxford, 1990.
(35) Loh, S. K.; Hales, D. A.; Lian, L.; Armentrout, P. B. *J. Chem. Phys.* **1989**, *90*, 5466.
(36) Waage, E. V.; Rabinovitch, B. S. *Chem. Rev.* **1970**, *70*, 377.
(37) Chesnavich, W. J.; Bowers, M. T. *J. Phys. Chem.* **1979**, *83*, 900.
(38) Armentrout, P. B. In *Advances in Gas Phase Ion Chemistry*; Adams, N. G., Babcock, L. M., Eds.; JAI: Greenwich, 1992; Vol. 1, pp 83−119.
(39) See, for example: Sunderlin, L. S.; Armentrout, P. B. *Int. J. Mass Spectrom. Ion Processes* **1989**, *94*, 149.
(40) See, for example, Figure 1 in ref 4.
(41) Armentrout, P. B.; Simons, J. *J. Am. Chem. Soc.* **1992**, *114*, 8627.
(42) *Chemical Thermodynamics*; Rock, P. A., Ed.; University Science Books: Mill Valley, CA, 1983; Chapter 14.
(43) Anvia, F.; Walsh, S.; Capon, M.; Koppel, I. A.; Taft, R. W.; de Paz, J. L. G.; Catalan, J. *J. Am. Chem. Soc.* **1990**, *112*, 5095.
(44) Feller, D.; Glendening, E. D.; Kendall, R. A.; Peterson, K. A. *J. Chem. Phys.* **1994**, *100*, 4981.
(45) Lias, S. G.; Liebman, J. F.; Levin, R. D. *J. Phys. Chem. Ref. Data* **1984**, *13*, 695. The value for PA(2-methyl-1-propanol) is assumed to equal that of PA(2-propanol) as indicated by: Taft, R. W.; Taagepera, M.; Abboud, J. L. M.; Wolf, J. F.; DeFrees, D. J.; Hehre, W. J.; Bartmess, J. E.; McIver, R. T. *J. Am. Chem. Soc.* **1978**, *100*, 7765. The value for PA(2-butanol) is estimated by assuming that the methyl substituent effect in going from 2-propanol to 2-butanol is equivalent to that going from ethanol to 1-propanol, 10.5 kJ/mol.
(46) In the butanol systems, we might also have expected to see decomposition of the $C_4H_9^+$ product by loss of methane to yield $C_3H_5^+$; unfortunately, this product was masked by ArH^+, a product formed very efficiently by CID of Ar_2H^+. This ion, which has the same mass as Li^+-(butanol), was about a 1% impurity in the desired ion beams and clearly will not interfere with the measurements of any other products.
(47) Meyer, F.; Khan, F. A.; Armentrout, P. B. *J. Am. Chem. Soc.* **1995**, *117*, 9740.
(48) Lifshitz, C. *Adv. Mass Spectrom.* **1989**, *11*, 113.
(49) Allison, J.; Ridge, D. P. *J. Am. Chem. Soc.* **1979**, *101*, 4998.
(50) Creasy, W. R.; Farrar, J. M. *J. Phys. Chem.* **1985**, *89*, 3952; *J. Chem. Phys.* **1986**, *85*, 162.
(51) Gioumousis, G.; Stevenson, D. P. *J. Chem. Phys.* **1958**, *29*, 294.
(52) *Molecular Reaction Dynamics*; Levine, R. D., Bernstein, R. B., Eds.; Oxford University: New York, 1974; p 136.